Paper: ASAT-15-025-CA

15th International Conference on
AEROSPACE SCIENCES & AVIATION TECHNOLOGY,
ASAT - 15 – May 28 - 30, 2013, Email: asat@mtc.edu.eg ,
Military Technical College, Kobry Elkobbah, Cairo, Egypt,
Tel: +(202) 24025292 –24036138, Fax: +(202) 22621908

Novel Cationic Gemini Surfactants with Different Chain Lengths as Corrosion Inhibitors for Carbon Steel in 1 M HCl

{M. I. Nessim, O. A. A. Elshamy, O. H. Abdelraheem*, and M. M. Osman}†

Abstract: Three cationic gemini surfactants of the type N^2,N^3-dialkyl-N^2,N^2,N^3,N^3-tetramethylbutane diamminium bromide namely Ia, Ib and Ic have been synthesized. Their chemical structures were elucidated by the routine methodologies ^{1}H-NMR, elemental analysis and mass spectroscopy. The surface active properties were examined and found to be influenced by the chemical structure of the surfactants. The synthesized cationic gemini surfactants were tested as corrosion inhibitors for pipeline carbon steel API 5LX52 immersed in 1 M HCl solution, using weight loss method. The obtained data refer to very good inhibitive efficiencies vary with concentrations, and increase in the following order: Ia >Ib > Ic. The Quantum chemical parameters such as highest occupied molecular orbital (HOMO), lowest unoccupied molecular orbital (LUMO) energy levels, energy gap (E_{HOMO}-E_{LUMO}), the dipole moment and charge densities were calculated. The theoretical calculations were in good agreement with corrosion inhibition results.

Keywords: Gemini surfactants; Corrosion inhibition; Carbon steel; Weight loss; Surface activities and Quantum chemical parameters.

1. Introduction

The application of surfactants as corrosion inhibitors has been studied extensively [1]. Dimeric (gemini) surfactants are a kind of surfactants made up of two identical amphiphilic moieties connected to the level of the head groups by a spacer group, rather than one hydrophilic group and one hydrophobic group for conventional surfactants [2-5]. Indeed, they offer some advantages, such as lower micelle concentration (CMC), higher surface activity and better wetting properties than the corresponding monomeric surfactants [6-11]. Owing to these unique properties, gemini surfactants have been widely used in industrial detergency, gelation of organic solvents, template synthesis of various materials, etc, [12-13]. Therefore, investigation on gemini surfactants is still an attractive subject for research. Considerable efforts have been made to design surfactants, and most of them have been focused on the effect of spacer length or its flexibility and hydophobicity [14-15]. In order to evaluate compounds as corrosion inhibitors and to design novel inhibitors, much more research works were concentrated on the studies of the relationship between structural characteristics of the organic compounds and their inhibiting effects [16].

Quantum chemical methods have already proven to be very useful in determining the molecular structure as well as elucidating the electronic structure and reactivity. Thus, it has become a common practice to carry out quantum chemical calculations in corrosion inhibition

* omnia_hassan55@yahoo.com

† Analysis and Evaluation Department, Egyptian Petroleum Research Institute (EPRI).1, Ahmed El- Zomor St., Nasr City 11727 Cairo, Egypt.

studies. The concept of assessing the efficiency of a corrosion inhibitor with the help of computational chemistry is to search for compounds with desired properties using chemical intuition and experience into a mathematically quantified and computerized form [17-18].
The first goal of this work was to design a series of N^2,N^3-dialkyl-N^2,N^2,N^3,N^3-tetramethylbutane diamminium bromide cationic gemini surfactants, featured with a branched spacer and to investigate their surface activity properties. The second one is to study the inhibitive effect of these surfactants as corrosion inhibitors for carbon steel in 1 M HCl and discussing the results in the light of the theoretical quantum chemical calculations.

2. Experimental Methods and Materials

2.1 Synthesis

A series of cationic gemini surfactants of the type N^2,N^3-dialkyl-N^2,N^2,N^3,N^3-tetramethylbutane diaminium bromide namely as Ia, Ib and Ic; (where the alkyl group is dodecyl-, tetradecyl- and hexadecyl- respectively) were synthesized. A mixture of 2,3-dibromobutane (0.05 mol) and N,N-dimethylalkylamine (0.0625 mol), is heated in absolute ethanol under reflux for 24 hours, then ethanol is evaporated using the rotary evaporating system. the product was waxy white (due to the presence of the amine in excess). The excess amine was removed by extraction with a mixture of ether-benzene, and finally by an extraction with hexane.
The resulting pure product was recrystallized in pure acetone. The resulting products were confirmed by elemental analysis (Table 1), ^{1}H-NMR (Table 2) and mass spectroscopy (Table 3a,b,c). The molecular structure of compounds is shown in Fig.1, where n equals (9,11,13) for Ia, Ib, Ic respectively.

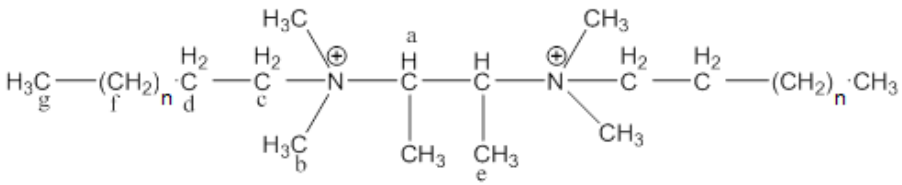

Fig. 1. Molecular structure of synthesized cationic gemini surfactants

Table 1. Elemental analysis of compounds Ia, Ib and Ic

Element %	C%		H%		Br%		N%	
Surfactant	Calc.	Obs.	Calc.	Obs.	Calc.	Obs.	Calc.	Obs.
Ia	59.81	59.58	10.90	10.72	24.92	24.95	4.36	4.75
Ib	61.87	61.85	11.25	11.40	22.89	22.67	4.01	4.08
Ic	63.64	63.45	11.48	11.52	21.17	21.36	3.71	3.65

2.2 Measurement of Surface Tension

The surface tension, at air/liquid interface, of the three synthesized cationic gemini surfactants was determined at 35ºC, measured using De-Nouy Tensiometer (Kruss K6 type) which calibrated against distilled water (specific conductivity 1.1×10^{-6} ohm^{-1} cm^{-1} at 30°C) [19]. Freshly prepared aqueous solution of the surfactants (Ia, Ib and Ic), in deionized water was prepared with a concentration range 0.01-10 mmol/L.

Table 2. ^{1}H-NMR spectroscopy of Ia, Ib and Ic

Type of proton	Chemical Shift (δ) ppm	Spin multiplicity
a	3.88	Quartet
b	3.44	Singlet
c	3.32	Triplet
d	2.09	Multiplet
e	1.66	Doublet
f	1.22	Multiplet
g	0.86	Triplet

Table 3a Mass spectroscopy of m/z 642 ($C_{32}H_{70}Br_2N_2$)

m/z	Molecular Formula	m/z	Molecular formula
642	$C_{32}H_{70}Br_2N_2]^{3+}$.	253	$C_{16}H_{33}N_2]^{3+.}$
482	$C_{32}H_{70}N_2]^{3+.}$	211	$C_{14}H_{29}N]^{2+.}$
467	$C_{31}H_{67}N_2]^{3+.}$	98	$C_6H_{12}N]^{2+.}$
452	$C_{30}H_{64}N_2]^{3+.}$	43	$C_2H_5N]^{2+.}$
283	$C_{18}H_{39}N_2]^{3+.}$	29	$CH_2N]^{2+.}$
268	$C_{17}H_{36}N_2]^{3+.}$		

Table 3b Mass spectroscopy of Ib m/z 698 ($C_{36}H_{78}Br_2N_2$)

m/z	Molecular Formula	m/z	Molecular formula
698	$C_{36}H+Br_2N_2]^{3+.}$	283	$C_{18}H_{37}N_2]^{3+.}$
538	$C_{36}H_{78}N_2]^{3+.}$	241	$C_{16}H_{25}N]^{2+.}$
525	$C_{35}H_{75}N_2]^{3+.}$	98	$C_6H_{12}N]^{2+.}$
510	$C_{34}H_{72}N_2]^{3+.}$	43	$C_2H_5N]^{2+.}$
313	$C_{20}H_{43}N_2]^{3+.}$	29	$CH_2N]^{2+.}$
298	$C_{19}H_{40}N_2]^{3+.}$		

Table 3c Mass spectroscopy of Ic m/z 754 ($C_{40}H_{86}Br_2N_2$)

m/z	Molecular Formula	m/z	Molecular formula
754	$C_{40}H_{86}Br_2N_2]^{3+.}$	309	$C_{20}H_{41}N_2]^{3+.}$
594	$C_{40}H_{86}N_2]^{3+.}$	267	$C_{18}H_{37}N]^{2+.}$
579	$C_{39}H_{83}N_2]^{3+.}$	98	$C_6H_{12}N]^{2+.}$
564	$C_{38}H_{80}N_2]^{3+.}$	43	$C_2H_5N]^{2+.}$
339	$C_{22}H_{47}N_2]^{3+.}$	29	$CH_2N]^{2+.}$
324	$C_{21}H_{44}N_2]^{3+.}$		

2.3 Weight Loss Measurements

Specimens of low carbon steel with dimensions (1cm × 1cm × 0.5cm) were used. Carbon steel grade is (API 5L X52) with chemical composition C: 0.28%, Si: 0.24%, Mn: 1.24%, P: 0.013%, Cr: 0.02%, Ni: 0.02%, Al: 0.03% and the rest is Fe. Prior to immersion, the specimens were abraded in sequence using emery papers of grade number 220, 320, 400, 600, 800, 1000 and 1200. The samples were allowed to stand for 72 hr in 1M HCl solution in the absence and presence of different concentrations of inhibitors ranged from 4×10^{-5} to 4×10^{-3} mol.l^{-1}. All tests are run in duplicate and the calculated weight losses are averaged.

2.4 Quantum Chemical Calculations

Quantum mechanical program Chem Bio Draw Ultra 12, was used for molecular modeling. The calculations were based on Ab initio (HF/3-21G and MP2/3-21G) and semiemperical (MNDO, AM1 and PM3) methods.

3 Results and Discussion

3.1 Surface Properties

The critical micelle concentrations CMC of the investigated surfactants were determined at 35ºC by plotting the surface tension in mN m^{-1}, versus log concentration as shown in Fig.2. The abrupt change in the linear line was taken as a critical micelle concentration. The CMC values together with other surface parameters are listed in Table 4. By careful inspection CMC decreases as the hydrophobicity increases.

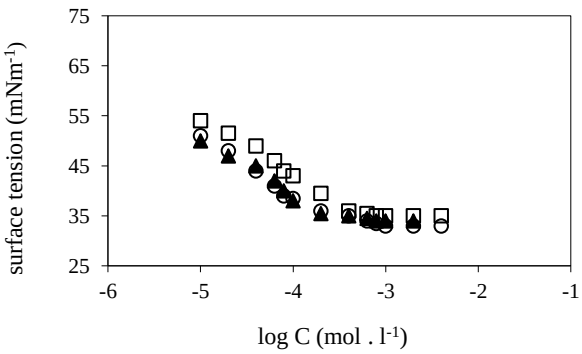

(▲) Ia; (o) Ib; and (□) Ic.

Fig. 2. Variation of surface tension with log C

Table 4. Surface properties of the synthesized gemini surfactants

Surfactants	CMC×10^4	Γ_{max} ×10^{10}	Amin	Π
Ia	4.89	1.83	0.91	34.50
Ib	4.47	3.75	0.44	30.50
Ic	3.16	4.24	0.39	28.50

The surface excess concentration Γ_{max} (mol /cm^2) by applying Gibbs equation [20].

$$\Gamma_{max} = - \frac{1}{2.303nRT} \frac{d\gamma}{dlogC} \quad (1)$$

where R is the gas constant (8.314 J/mol) and T is the absolute temperature. The constant n takes value equals 2 for an ionic surfactants, were the surfactant ion and the counter ion are

univalent, and n=3 for a dimeric surfactant made up of divalent surfactant ion and two univalent counter ions, in absence of swamping electrolyte [21].
The Γ_{max} values in Table 4 were used to calculate the minimum area per molecule, A_{min} in $Å^2$/molecule at the aqueous phase interface using the relationship:

$$A_{min} = \frac{10^{16}}{N_A \Gamma_{max}} \quad (2)$$

where, N_A: Avogadro's number, $6.023 \times 10_{23}$. There was slight increase in Γ_{max} and decrease in A_{min} by increase in the hydrophobic chain length which might be caused from increasing van der Vaals interaction. The effectiveness (π_{cmc}), which indicate the surface activity of the surfactants molecules at their CMCs were determined. The effectiveness in surface tension reduction (π_{cmc}) of the prepared surfactants at 35ºC revealed that Ia has the higher value.

3.2 Weight Loss Measurements

The inhibition efficiency E%. was determined by the following equation [22]:

$$\theta = 1 - (\Delta Wi / \Delta Wo) \quad (3)$$

$$E\ \% = 1 - (\Delta Wi / \Delta Wo) \times 100 \quad (4)$$

where E% is the corrosion inhibition efficiency, θ is coverage of the metal surface and ΔW_o and ΔW_i are the weight loss per unit area in absence and presence of inhibitors respectively. The results listed in Table 5. The plotting of surface coverage (θ) against log C illustrated in Fig 4. The corrosion rate is a concentration dependent, where efficiency (E%) increases with increasing inhibitors concentration and reaches the maximum value near CMC. The inhibition efficiency found to be ranked as follows, Ia> Ib > Ic. It means that the efficiency decreases by increasing the tail chain length of the synthesized gemini surfactants with branched spacer.

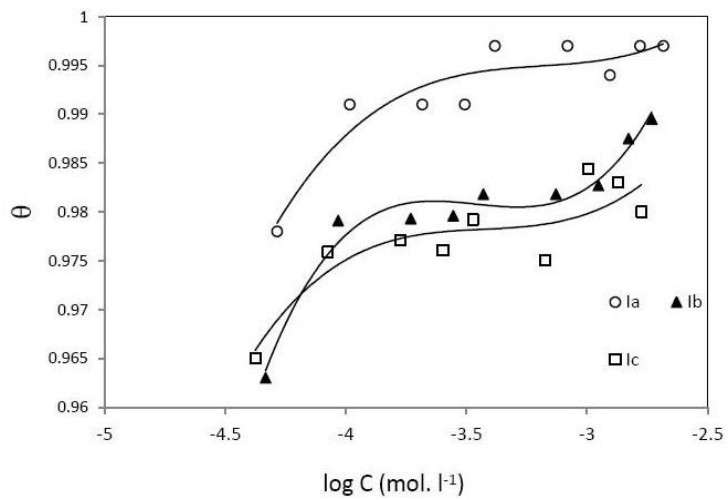

Fig. 3 Variation of the inhibition efficiency of carbon steel in the presence of different concentrations of the inhibitors

The inhibitors having θ near unity, is indicating almost a full coverage of the metal surface with adsorbed surfactant molecules as a good physical barrier shielding the corroding surface from the corrosive medium. From surface activity measurements (Table 4), the greatest effectiveness in surface tension reduction (π_{cmc}) was achieved by Ia compared with that obtained by the other two surfactants, which may explain the highest inhibition efficiency achieved by Ia.

Table 5 The corrosion inhibition and surface coverage of carbon steel in 1 M HCl with addition of surfactants Ia, Ib and Ic

Surfactants	Conc. (mol.l^{-1})	θ	E %
Ia	4×10^{-5}	0.9780	97.80
	1×10^{-4}	0.9910	99.10
	2×10^{-4}	0.9910	99.10
	3×10^{-4}	0.9910	99.10
	4×10^{-4}	0.9970	99.70
	8×10^{-4}	0.9970	99.70
	1×10^{-3}	0.9940	99.40
	2×10^{-3}	0.9970	99.70
	4×10^{-3}	0.9970	99.70
Ib	4×10^{-5}	0.9630	96.30
	1×10^{-4}	0.9791	97.91
	2×10^{-4}	0.9793	97.93
	3×10^{-4}	0.9796	97.96
	4×10^{-4}	0.9818	98.18
	8×10^{-4}	0.9818	98.18
	1×10^{-3}	0.9827	98.27
	2×10^{-3}	0.9875	98.75
	4×10^{-3}	0.9895	98.95
Ic	4×10^{-5}	0.9650	96.50
	1×10^{-4}	0.9759	97.59
	2×10^{-4}	0.9771	97.71
	3×10^{-4}	0.9760	97.60
	4×10^{-4}	0.9792	97.92
	8×10^{-4}	0.9750	97.50
	1×10^{-3}	0.9844	98.44
	2×10^{-3}	0.9830	98.30
	4×10^{-3}	0.9800	98.00

3.3 Adsorption Isotherm

The inhibition efficiency has been found to be closely related to inhibitor adsorption abilities and molecular properties for different kinds of organic compounds [23]. In order to determine the adsorption mode, various isotherms were tested and by far the best fit was obtained with the Langmuir isotherm Fig. 4. by the following relation [24]:

$$\frac{C}{\theta} = \frac{1}{Kads} + C \qquad (5)$$

where C is the concentration of the inhibitor, Θ is the surface coverage and K_{ads} is the equilibrium adsorption constant Table 6. shows the parameters and the regression factor calculated from Langmuir adsorption isotherm. All correlation coefficients (r^2) exceeded 0.99 indicates that the corrosion inhibition of carbon steel by the prepared cationic gemini

surfactants was attributed to adsorption of these compounds on the metal surface. However, the slopes of the C/ θ versus C plots show a little deviation from unity, This deviation may be explained on the basis of interaction between the adsorbed species on the metal surface by mutual repulsion or attraction [25].
High values of the adsorption constant K_{ads} can be reasoned for better adsorption and high inhibition efficiency [26], which is consistent with data obtained from weight loss investigations.

Table 6. Adsorption parameters of inhibitors surfactants on the steel surface.

Surfactant	Linear correlation coefficient, r^2	Slope	Kads (l. mol^{-1})
Ia	0.9999	1.0028	98.3768×10^4
Ib	0.9999	1.0110	97.6685×10^4
Ic	0.9999	1.0183	90.0556×10^4

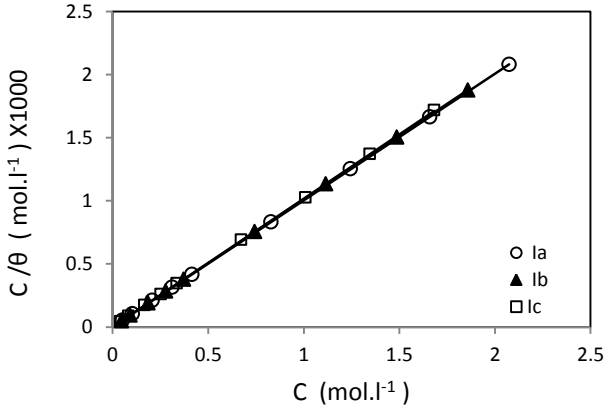

Fig. 4. Langmuir isotherm plots for carbon steel in 1M HCl at presence of different concentrations of cationic gemini surfactants Ia, Ib and Ic.

3.4 Quantum Chemical Calculations

Using the Ab initio (HF/3-21G and MP2/3-21G) and semiempirical (AM1, MNDO and PM3) methods of calculations by Chem Bio Draw Ultra 12 software, the Huckel and Mulliken charges, the dipole moments, E_{HOMO} (the highest occupied molecular orbital) and E_{LUMO} (the lowest unoccupied molecular orbital) values were calculated. The charges representative atoms and other relevant quantum parameters were listed in Tables 7,8 and 9. The optimized structure of the molecules and the electric/orbital density distributions of HOMO and LUMO are illustrated in Fig.5 and Fig.6 respectively.
Mulliken population analysis is mostly used for the calculation of the charge distribution in a molecule [27]. These numerical quantities are easy to obtain and they provide at least a qualitative understanding of the structure and reactivity of molecules [28]. Furthermore, atomic charges are used for the description of the molecular polarity of molecules. By careful examination of Tables 7,8 and 9, it is found that the values of the electronegative charges of the N13, N15, N16, N17, N18, and N20, were irrelevant to the inhibition efficiency. These

results suggested that the adsorptions might not be attributed to a chemical bond between the electronegative atoms and the metal surface.

The dipole moment (μ) values were founded to be increased by the increase in the hydrophobic chain length. It may indicated that the adsorptions might not be arisen from intermolecular electrostatic force [16]. Highest occupied molecular orbital energy (E_{HOMO}) and lowest unoccupied molecular orbital energy (E_{LUMO}) are very popular quantum chemical parameters. These orbitals, also called the frontier orbitals, determine the way the molecule interacts with other species. The HOMO is the orbital that could act as an electron donor, since it is the outermost (highest energy) orbital containing electrons. The LUMO is the orbital that could act as the electron acceptor, since it is the innermost (lowest energy) orbital that has room to accept electrons. According to the frontier molecular orbital theory, the formation of a transition state is due to an interaction between the frontier orbitals (HOMO and LUMO) of reactants [29].

Table 7 Quantum Chemical Parameters of Ia

Quantum parameters	HF(3-21G)	MP2(3-21G)	AM1	MNDO	PM3
E_{HOMO} (eV)	23.790	23.778	23.776	23.783	23.781
E_{LUMO} (eV)	25.736	25.741	25.740	25.741	25.739
$E_{LUMO-HOMO}$ (eV)	01.946	01.963	01.964	01.958	01.958
Huckel charge (eV)	N_{13} = 0.4906 N_{16} = 0.4867	N_{13} = 0.4915 N_{16}= 0.4871	N_{13} = 0.4907 N_{16} = 0.4864	N_{13} = 0.4908 N_{16} = 0.4868	N_{13} = 0.4910 N_{16} = 0.4873
Mulliken charge (eV)	N_{13} = -0.7385 N_{16} = -0.7390	N_{13} = -0.7423 N_{16} = -0.7395	N_{13} = 0.0191 N_{16} = 0.0301	N_{13} = -0.1068 N_{16} = -0.0979	N_{13} = 0.5958 N_{16}= 0.6185
μ (Debye)	29.67	29.47	29.97	31.03	30.33

Table 8 Quantum chemical parameters of Ib

Quantum parameters	HF(3-21G)	MP2/3-21G	AM1	MNDO	PM3
E_{HOMO} (eV)	23.778	23.778	23.779	23.780	23.784
E_{LUMO} (eV)	25.737	25.739	25.747	25.746	25.745
$E_{LUMO-HOMO}$ (eV)	1.959	01.961	1.968	1.966	1.961
Huckel charge (ev)	N_{15} = 0.4913 N_{18} = 0.4877	N_{15} = 0.4912 N_{18} = 0.4872	N_{15} = 0.5542 N_{18} = 0.6502	N_{15} = 0.4912 N_{18} = 0.4876	N_{15} = 0.4574 N_{18} = 0.4926
Mulliken charge(ev)	N_{15} = -0.7398 N_{18} = -0.7403	N_{15} = -0.7424 N_{13} = -0.7379	N_{15} = 0.0179 N_{18} = 0.0304	N_{15} = -0.1068 N_{18} = -0.0983	N_{15} = 0.5587 N_{18} = 0.5857
μ (Debye)	36.74	36.71	36.99	38.17	37.59

Table 9 Quantum chemical parameters of Ic

Quantum parameters	HF(3-21G)	MP2/3-21G	AM1	MNDO	PM3
E_{HOMO} (eV)	23.774	23.774	23.760	23.767	23.778
E_{LUMO} (eV)	25.739	25.743	25.734	25.741	25.746
$E_{LUMO-HOMO}$ (eV)	1.965	1.969	1.974	1.974	1.968
Huckel charge (eV)	N_{17} = 0.4906 N_{20} = 0.4874	N_{17} = 0.4857 N_{20} = 0.4746	N_{17} = 0.4904 N_{20} = 0.4874	N_{17} = 0.4904 N_{20} = 0.4871	N_{17} = 0.4526 N_{20} = 0.4921
Mulliken charge (eV)	N_{17} = -0.7396 N_{20} = -0.7103	N_{17} = -0.7411 N_{20} = -0.7378	N_{17} = -0.0191 N_{20}= -0.0302	N_{17} = -0.1068 N_{20} = -0.0978	N_{17} = 0.5581 N_{20} = 0.5843
μ (Debye)	43.93	44.36	44.35	45.43	44.87

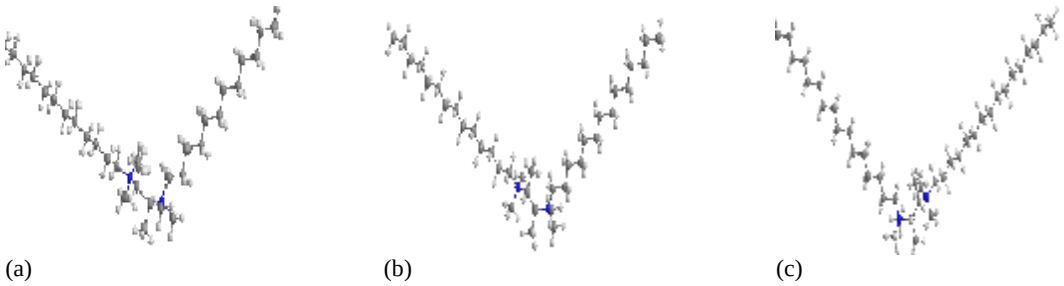

Fig. 5. Optimized structure of the synthesized cationic gemini surfactants of the type N^2,N^3-dialkyl-N^2,N^2,N^3,N^3-tetramethylbutane diamminium bromide: (a) Ia; (b) Ib; (c) Ic

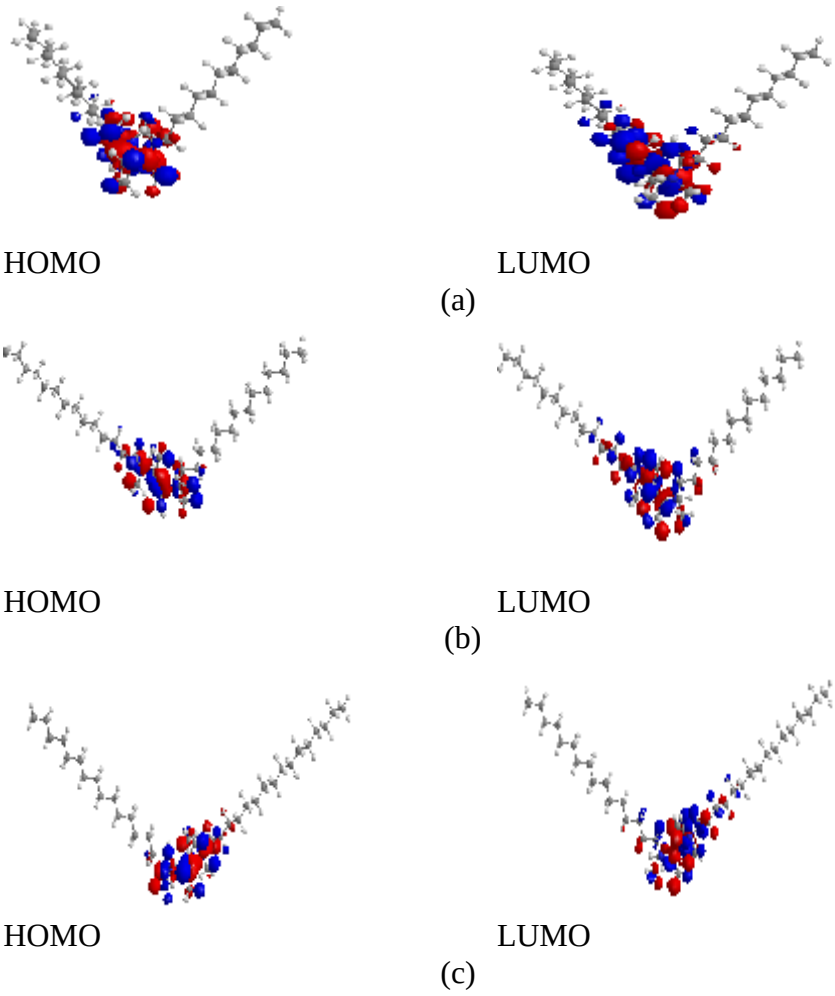

Fig. 6. The frontier molecule orbital density distributions of the prepared three cationic gemini surfactants of the type N^2,N^3-dialkyl-N^2,N^2,N^3,N^3-tetramethylbutane diamminium bromide: (a) Ia; (b) Ib; (c) Ic.

From Tables 6, 7 and 8 it is found that the E_{HOMO} and the E_{LUMO} changed rulelessly, while the energy gap E_{LUMO}- E_{HOMO}; the difference in energy between the E_{HOMO} and E_{LUMO} decreased with increasing the inhibition efficiency. The energy gap (ΔE) is an important stability index [30]. A large HOMO–LUMO gap implies high stability for the molecule in chemical reactions [31].

The values of (*ΔE*) indicates remarkably that the smaller energy gap results in a high corrosion inhibition, reflecting the stronger interaction between the inhibitors and metal surface. The interactions are probably physical adsorption [32-34].
An attempt to search correlations among the experimentally obtained inhibition efficiency results and theoretically calculated quantum parameter; energy gap (*ΔE*) values; are illustrated in Fig.7. The plotting shows that the best correlation obtained using semi empirical methods MNDO and AM1. This result is in accordance with other works [18, 23, 35 and 36].

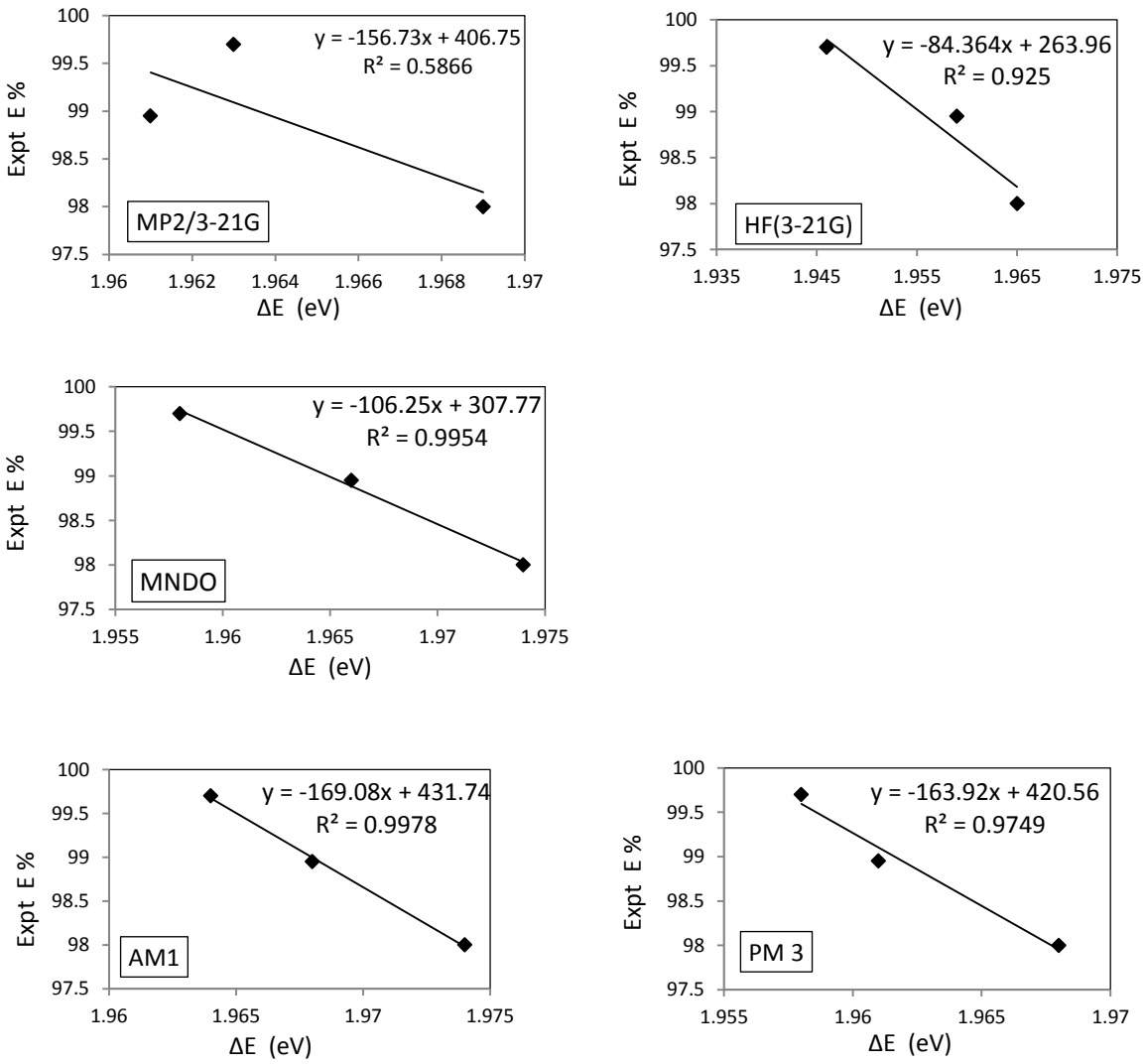

Fig. 7 Correlations between experimental %E and calculated quantum chemical parameter (ΔE).

4. Conclusions

Novel synthesized cationic gemini surfactants featured with a branched spacer ,showed good inhibition properties for the corrosion of pipeline carbon steel API X52 in 1 M HCl solutions, and the inhibition efficiency increased as their concentration increases.
Based on the weight loss measurements, the inhibiting efficiencies of cationic gemini surfactants followed the order of Ia > Ib > Ic, which is the same order of effectivness in surface tension reduction.
The adsorption of studied cationic gemini surfactants on the carbon steel obeyed the Langmuir adsorption isotherm model.

The experimentally obtained inhibition efficiency was correlated with energy gap which is theoretically calculated by quantum chemical calculations. The correlation was well-proportioned suggested the adsorption of synthesized cationic gemini surfactants on the carbon steel was physical adsorption.

5. References

[1] L. Qiu A. Xie, Y. Shen, Applied Surface Science ,246,1 (2005).
[2] L.Grosmaire, M. Chorro, C. Chorro, S. Partyka, R. Zana, , Colloid Polym. Sci. ,115,31 (2000).
[3] R. Zana, , Adv. Colloid interface Sci., 97, 205 (2002).
[4] M. Pisarcik, M.J. Rosen, M. Polakovicova, F. Devinsky, I. Lacko, , J. Colloid interface Sci., 289, 560 (2005).
[5] Y.X. Wang, Y.C. Han, X. Huang, M.W. Cao, Y.L. Wang, , J. Colloid interface Sci., 319, 534 (2008).
[6] Zana, M. Benrraou, R. Rueff, Lngmuir, 7, 1072 (1991).
[7] C. Chorro, M. Chorro, O. Dolladille, S. Partyka, R. Zana, J. Colloid interface Sci., 199, 169 (1998).
[8] R. Oda, I. Huc, S.J. Canadau, Chem. Commun., 2105, (1997).
[9] F.L. Duivenvoorde, M.C. Feiters, S.J. van der Gaast, J.B.F.N. Engberts, Langmuir ,13, 3737 (1997).
[10] R. Zana, J.D. Xia, in: R. Zana, J.D. Xia (Eds.), Gemini Surfactants, Dekker, New York, (2004).
[11] T. Lu, F. Han, G.R. Mao, G.F. Lin, J.B. Huang, X. Huang, Y.L. Wang, H.L. Fu, Langmuir, 23, 2932 (2007).
[12] S.H. Han, J. Xu, W.G. Hou, X.M. Yu, Y.S. Wang, J. Phys. Chem. B ,108, 15043 (2004).
[13] T. Lu, Y. Lan, Ch. Liu, J. Huang, Y. Wan, J. Colloid Interface Si., 377, 222 (2012).
[14] L. Grosmaire, M. Chorro, C. Chorro, S. Partyka, R. Zana, , Prog Colloid Polym. Sci,. 115, 31 (2000).
[15] L. Grosmaire, M. Chorro, C. Chorro, S. Partyka, S. Lagerge,, Thermocheimica Acta, 379, 255 (2001).
[16] Y. Yan, W. Li , L. Cai, B. Hou, Electrochimica Acta, 53, 5953 (2008).
[17] E. Kraka, D. Cremer, J. Am. Chem. Soc.,122, 8245 (2000).
[18] G. Gece, Corrosion Science, 50, 2981 (2008).
[19] M.J. Rosen, M.L. Baum and F. Kasher, JAOCS, 53, 742 (1976).
[20] M.J. Rosen, Surfactants and Interfacial phenomena. John Wiley & Sons, New York (1978).
[21] E. Alami, S. Abrahmsen-Alami, J. Eastoe, R.K. Heenan, , Langmuir, 19 (2003) 1821.
[22] A.M.Badawi, M.A.Hegazy, A.A.El-Sawy, H.M.Ahmed ,W.W.Kamel, Marerials Chemistry and Physics, 124,458 (2010).
[23] T. Arslan, F. Kandemirli , E.E. Ebenso, I. Love, H. Alemu, Corrosion Science, 51, 35 (2009).
[24] A.S. Fouda, A.A. Al-Sarawy, F.Sh. Ahmed, H.M. El-Abbasy Corrosion Science, Volume 51, Issue 3, 485 (2009).
[25] A.A Abdel-Azim., L.A Shalaby., H Abbas., Corros. Sci., 14, 21 (1974).
[26] M.A. Hegazy, Corrosion Science, 51,2610 (2009).
[27] J.N. Murrell, S.F. Kettle, J.M. Tedder, The Chemical Bond, John Wiley & Sons, Chichester, 1985.
[28] C. Gruber, V. Buss, Chemosphere, 19,1595 (1989).

[29] K. Fukui, Theory of Orientation and Stereoselection, Springer-Verlag, New York, (1975).
[30] D.F.V. Lewis, C. Ioannides, D.V. Parke, , Xenobiotica, 24,401 (1994).
[31] Z. Zhou, R.G. Parr, J. Am. Chem. Soc. ,112, 5720 (1990) .
[32] I. Lukovits, K. Palfi, E. Kalman, Corrosion 53, 915 (1997) .
[33] M. O¨ zcan, ˙I. Dehri, Prog. Org. Coat. 51, 181 (2004) .
[34] Y. Yana,,W. Li , L. Caia, B. Hou, Electrochimica Acta, 53, 5953 (2008).
[35] G.Bereket, E.Hür, C.Öğretir journal of molecular Structure (Theochem) 578, 79 (2002).
[36] I. Ahamad , R. Prasad , M.A. Quraishi, Corrosion Science, 52, 933 (2010).